Non-volatile phototransistor based on two dimensional $MoTe_2$ nanostructures

Kamoladdin Saidov[1,2*], *Khakimjan* Butanov[1], *Jamoliddin* Razzokov[1,3,4,5], *Shavkat* Mamatkulov[1], *Dong* Fang[6], and *Olim* Ruzimuradov[7,8]

[1]Institute of Material Science, Academy of Sciences of the Republic of Uzbekistan, Tashkent, Uzbekistan
[2]Tashkent State Technical University, Tashkent, Uzbekistan
[3]National University of Uzbekistan, Tashkent, Uzbekistan
[4]Akfa University, Tashkent, Uzbekistan
[5]"Tashkent Institute of Irrigation and Agricultural Mechanization Engineers" National Research University, Tashkent, Uzbekistan
[6]Kunming University of Science and Technology, Kunming, PR China
[7]Turin Polytechnic University in Tashkent, Tashkent, Uzbekistan
[8]National University of Uzbekistan, Tashkent, Uzbekistan

Abstract. We fabricate field-effect transistors (FETs) from low-layer molybdenum ditelluride (MoTe2) in the nanometer range and study its optoelectronic properties. In particular, we investigate the mechanisms of photocurrent generation in MoTe2 FETs using gate and bias-dependent photocurrent measurements. The results obtained show the photocurrent effects and signals generated in the MoTe2-electrode junctions, which identify the effect of amplifying the photoconductor in the off and on modes. This is different from those conventional MoTe2 FETs, which exhibited a continuous increase in photocurrent with no back gate voltage. These results play an important role in the fabrication of direction dependent field effect transistors based on MoTe2 crystals.

1 Introduction

Low dimensional materials have been exhibited exotic physical properties. Among them, transition-metal dichalcogenides (TMDs) layered semiconducting materials such as MoS_2, $MoSe_2$, $MoTe_2$, WS_2, WSe_2, WTe_2 and $PdSe_2$ have attracted great attention due to the possible candidate materials for the post-Si era [1]. The single layers of these 2D TMD nanomaterials [2] as a semiconductor have shown efficiency in light absorption, which leads to high responsivity of photodetectors [3]. The main technical characteristics of TMDs can be found in MX2 form. Here, M is a sheet that consists of hexagonal positioned order of atoms and this is stacked in between two layers of X atoms. Three layers of these crystals are sandwiched through the weak van der Waals forces which result the separation of the bulk crystals as a form of single 2D flakes [4]. The absence of covalent bonds between adjacent triple layers causes the shortage of dangling bonds in 2D TMD flakes.

*Corresponding author: k.saidov@skku.edu

This is the main reason for possessing a chemical stability and low carrier scattering on their surfaces. These kinds of layered TMD structures acquire a high anisotropy in their electrical properties [5, 6]. These qualities of semiconducting TMDs offer exceptional platforms for electronic and optoelectronic devices which is the root of next-generation FETs [7], light-emitting diodes, and Van der Waals heterostructure devices [8]. Besides, 2H-$MoTe_2$ also has been widely studied for applications in spin transport electronics and solar cells [9, 10]. In addition, both unipolar and ambipolar charge transport characteristics are the beneficial feature of single-layer and a-few-layer $MoTe_2$ FETs [11]. The polarity of these FETs can be easily tuned by means of the contact electrode [12].

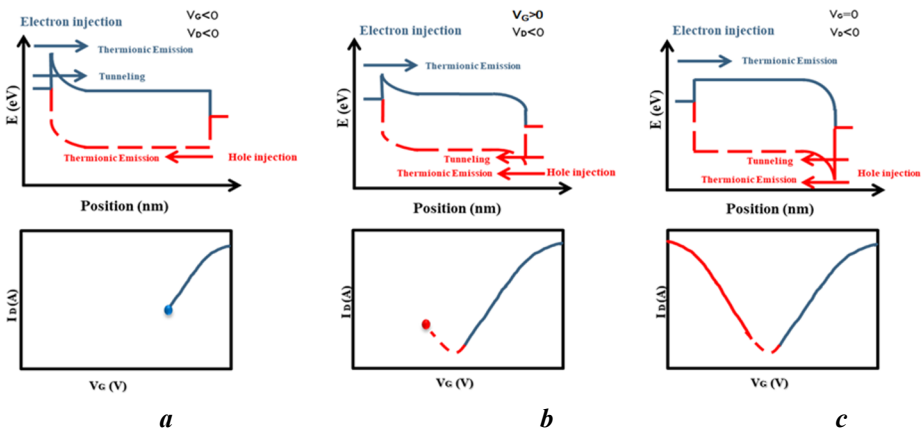

Fig. 1. Schematic view of ambipolar conduction: a) under the negative bias the electrons are injected, b) the gate bias is higher than zero and while the under bias, the holes are injected directly into the different carrier densities within the layers, c) the gate bias reached an equal to zero, the holes are fully injected and we might be seen an ambipolarity of the curve.

The applied external heat energy to the metal electrode leads to the thermionic emission on its surface. This in turn affects to the tunneling process which responsible for the flow of the current via the channel. I_{DS}-V_{BG} ambipolar transfer characteristic for normal edge contact TMDs, which are located near the charge transfer due to the difference in the Fermi levels of the metal and semiconductors (see Fig 1). As is clear from Fig.1 under the negative bias to the gate the injection of electrons into the $MoTe_2$ channel is taking place (see Fig. 1a), while under the positive bias the holes are injected (see Fig. 1b, c) [13, 14].

FETs are an essential component of many photodetector devices that we broadly use in research as well as in our daily life. Photodetector absorbs photons and converts them into electrical signals that can be further processed by standard electronics. The application of the latter includes spectral imaging, sensors, fiber optical communications, etc. The role of semiconducting 2D materials is quite important to enhance the functionality of photodetectors due to their transparency, high flexibility, and layer dependency tunable bandgaps [9, 13]. In contrast, the bulk silicon photodetectors experience due to the limitations as a light-absorbing material. The indirect bandgap of silicon is about 1.07 eV which limits the absorption of a visible and near-infrared range of the electromagnetic spectrum and as a result, the efficiency reduces [14]. In order to obtain high sensitivity, the silicon-based photodetectors need a thick channel which makes a photodetector quite compact. The electrical resistance of semiconductors decreases in photoconductive effect due to the generated excess free carriers in process of photon absorption [15]. The absence of illumination under the involvement of bias leads to the negligible flow of source-drain current. The exposure of materials to the light results in the absorption of photons which

causes the generation of e-h pairs and these pairs can be separated by the applied voltage (drain-source). Both photogenerated free electrons and holes travel towards opposite directions along the metal which affect an increase of current. The crossing of the channel occurs much faster in photogenerated electrons than the photogenerated holes in the case of slow mobility of holes in comparison to electron mobility [16]. Thus, many electrons can participate in the photocurrent originating the photoconductive gain which is characterized by the photogenerated carrier lifetime divided by the transit time [17]. Moreover, these electrons can be derived from a single photon, resulting in increased quantum efficiency [18, 19]. In previous studies, mainly the photoresponsivity of TMDs based FETs have been investigated [20, 22]. However, these results were obtained only for the of presents backgate sweep. In order to achieve better photoresponsivity, it is important to synthesize monolayer material that demonstrates higher charge transfer properties.

Here, we present the results of a thorough experimental study of photoresponsivity of $MoTe_2$ using Cr/Au metals as electrodes to shed light on the impact of Schottky barriers on the carrier transport characteristics of FETs [2, 23-25].

2 Experiment and Materials

The fabrication of the $MoTe_2$ phototransistor was prepared by using the dry-transfer method. Initially, the commercially available bulk material was used to extract a few layers i.e., of $MoTe_2$ flake. The flake was obtained by means of the mechanical exfoliating method and further used to place on Si wafer. Next, in order to transfer the $MoTe_2$ flake from the Si wafer into the pure Si/SiO_2 (300 nm) substrate the polyvinyl alcohol (PVA) was utilized. The exfoliated flakes were recognized using an optical microscope and characterized with an electrical measurement. The spin coater was used to coat the polymethyl methacrylate (PMMA) on top of $MoTe_2$. Thereafter, PVA was fully dissolved in water, while the $MoTe_2$ flake settled on the PMMA sheet. The Cr/Au electrodes were patterned using electron-beam evaporation of 5 nm Cr and 50 nm Au after the norm lift-off process. The output and transfer measurements were performed employing two-channel models which were applied the gate voltage. The AC photocurrent measurements we use to detect in the making small photocurrents with a low-noise current preamplifier (SR 570). The photocurrent and electrical measurements were fulfilled inside a Close Cycle Refrigerator (CCR) chamber. The chamber pressure inside was sustained at 1×10^{-7} Torr. Moreover, the chamber was equipped with a quartz window through which the applied laser could pass through and focus onto the sample. The green laser with 532 nm wavelength was directed to CCR which focused onto the sample is a partially suspended region. The chopper controller (Model SR540) provides a reference signal for the lock-in amplifier (SR 830) and detects simple voltages at a certain frequency of the modified light that affords a very sensitive measure of the photoresponse of these FET.

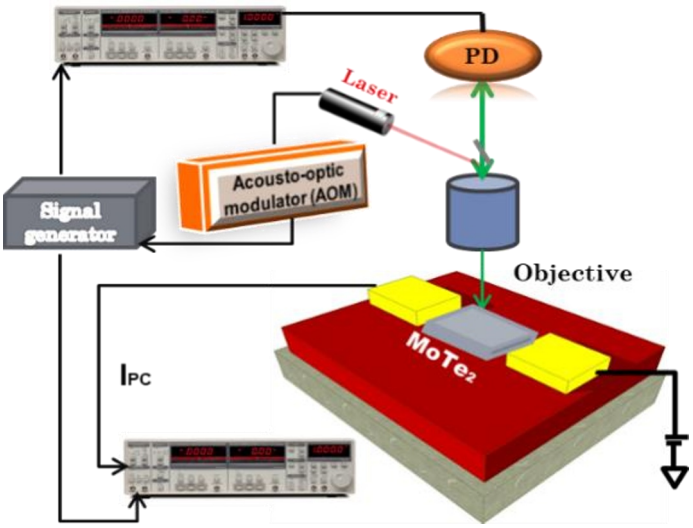

Fig. 2. The schematic circuit diagram of the experimental setup and device.

We propose a new structure of optoelectronic devices for ambipolar type FET based on a few and monolayer of TMD materials. The optoelectronic properties of a few layers of $MoTe_2$ *p-n* diodes were installed with scanning photocurrent microscopy (See, Fig. 2). We mainly concentrated on the p-type SiO_2 $MoTe_2$ FET devices in our experimental measurements. P - and n-type parameters of $MoTe_2$ FET devices can be determined by current-voltage (I-V) measurements of FET. The I-V characteristics were measured using the six probe station and Keithly 4200-SCS's Source Measure Units (SMUs) was employed as a source and measure both current and voltage. The lower gate voltage can lead to a higher Schottky barrier height between metal and channel.

3 Results and discussion

The electric transport measurements were performed in a wide range of source-drain voltage bias values. The Si substrate was used as a back-gate source which applied a voltage-bias in the range of +60 to -60 V. Fig. 3 illustrates a) the schematic structure of fabricated $MoTe_2$ and b) photo-optical response of the device junction with the few-layer film deposited onto a 300 nm SiO_2/Si substrate.

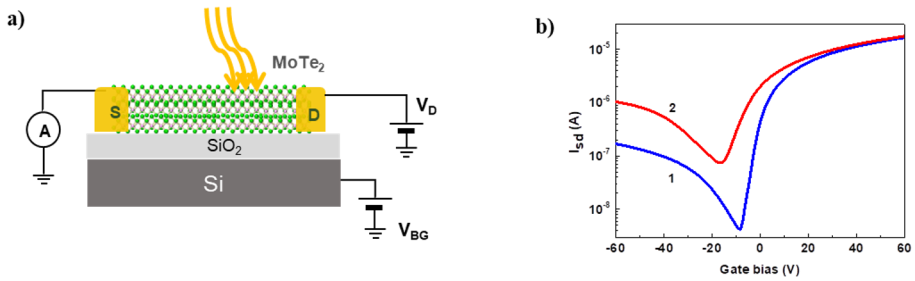

Fig. 3. a) Schematic view of the $MoTe_2$ FET and measurement setup. b) The current vs. gate voltage characteristics in the dark (blue curve -1) and under illumination by laser irradiation (red curve -2)

It is clear from Fig. 3(b) that our $MoTe_2$ FET demonstrates the ambipolar conduction behavior in the dark as well as under illumination conditions. In order to understand the ambipolar conduction of FET, a theoretical model was proposed in the literature [26]. The AC photocurrent and electrical performance of FET devices mainly depend on the metal electrodes junction [22, 27]. In the next stage, the time-resolved photoresponse technique was employed to assess the trap states. In addition, the device is subjected to the air to introduce the surface trap states on $MoTe_2$. The reason for emerging a surface trap state might be due to the sample size which is comparatively thicker. This potentiates less chance for the photoexcited carrier to be trapped at the dielectric interface in monolayer devices in comparison to the few layers one.

We mapped out the photocurrent spreading in the channel region of the 15-layered $MoTe_2$ device and further, the trap states have been also estimated. The maximum trap density is observed to be about 6×10^{12} cm^{-2}. Since the bandgap of the $MoTe_2$ remained unaltered. It is expected that there will be inhomogeneity in trap density point-to-point, but overall the density remains the same. The variation of the photocurrent depending on the gate bias was in line with the previous results [28]. We performed a few measurements of the photocurrent and trap states by means of CCR devices as well. We obtained the same results during these measurements too which was eventually produces a small AC photocurrent (7 nA). Furthermore, we also determined the temperature-dependent transfer curves. As it was expected, the current level decreases on lowering the temperature, representing an actual characteristic of semiconductors. In addition, we also measured the output curves at 280 K by varying V_{gs}. The determined output curves were linear for the case of different V_{gs}. This points out that the Ohmic contact nature between $MoTe_2$ and Cr/Au electrode. Figure 4(a) demonstrates the schematics of the scanning photocurrent mapping of the $MoTe_2$ FET area (Fig. 4(b)) (the dimension is 8 x 5 µm) around the $MoTe_2$ structures at V_{bg} = 0V. Here, $MoTe_2$ was biased with V_{sd} = 1V and the photocurrent were measured through the channel. We observed a reduction of photocurrent close to the drain contact of $MoTe_2$ FET (see, the red region in Fig. 4(c)) in comparison to the channel part.

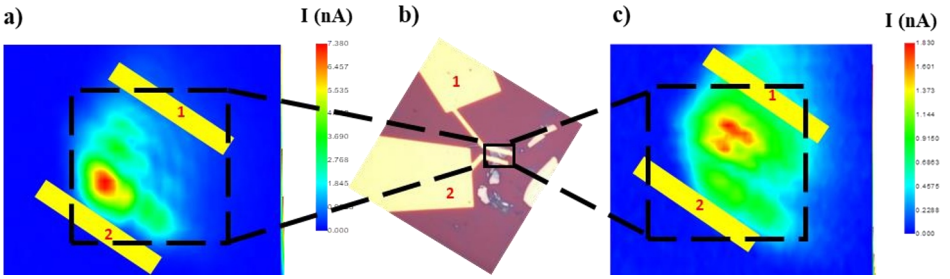

Fig. 4. (a) Photo current map of the transistor at V_{sd} = 1V and V_{bg} = 0V with laser power 9.5 µW/µm^2, black dashed line outlines the region of $MoTe_2$. (b) The optical image of $MoTe_2$ FET and (c) photo current map of the transistor at V_{sd} = 1V and V_{bg} = 60V with the same laser power

The values of photo-induced currents were varied from ~60 nA to 1 nA at $MoTe_2$ and SiO_2 substrate interface, respectively. During the exposure of laser, the emerged current dramatically increases up to 7~10 times (at V_{sd} = 1V) as schematically respresented in Fig. 4(a). The exposure of $MoTe_2$ to the beam laser leads to the photo-generated electrons and holes in photo-active $MoTe_2$. This consequently results in enhanced photo-current that is most likely due to the highly conductive interface which is easily separated by an applied electric field (V_{sd}). The optical view of the device is given in Fig. 4(b). The optoelectronic devices, specifically semiconductors mainly operate on the principle of direct electron-photon conversion which is a key process in the fields of photodetection and photovoltaic.[10]

Thus, the semiconductor's energy gap directly defines the energy efficiency scale of the device's optical excitation which is crucial for the fabrication of FETs.

4 Conclusions

Here, we performed opto-electrical measurements on freshly cleaved surfaces of $MoTe_2$ crystals in order to investigate their qualities. Particularly, the trap states were estimated for the case of 15-layered $MoTe_2$ and we found the maximum trap density being about 6×10^{12} cm^{-2}. Moreover, it is noteworthy that our $MoTe_2$ FET offers a higher AC photocurrent and on/off ratio in comparison with similar FETs [15, 21, 29, 30] which maintains the potential to increase the number of charges in photocurrent without gate sweeping.
$MoTe_2$ based device might perform an excellent stretchability without significant electrical performance degradation, which will be widely used in the near future for wearable and body-attachable electronics.

Acknowledgments

The authors are acknowledged for the financial support from the MID project MUK-2021-45; and FZ-2020092325 (Republic of Uzbekistan).

References

1. Novoselov, K. S. et al. Electric field effect in atomically thin carbon films. science 306, 666-669 (2004).
2. Razzokov, J., Marimuthu, P., Saidov, K., Ruzimuradov, O. & Mamatkulov, S. Penetration of Chitosan into the Single Walled Armchair Carbon Nanotubes: Atomic Scale Insight. Crystals 11, 1174 (2021).
3. Huang, C. et al. Lateral heterojunctions within monolayer MoSe 2–WSe 2 semiconductors. Nature materials 13, 1096-1101 (2014).
4. Novoselov, K. S. et al. Two-dimensional gas of massless Dirac fermions in graphene. nature 438, 197-200 (2005).
5. Lin, Y. F. et al. Ambipolar MoTe2 transistors and their applications in logic circuits. Advanced Materials 26, 3263-3269 (2014).
6. Novoselov, K. S. et al. Unconventional quantum Hall effect and Berry's phase of 2π in bilayer graphene. Nature physics 2, 177-180 (2006).
7. Novoselov, K. S. et al. Room-temperature quantum Hall effect in graphene. Science 315, 1379-1379 (2007).
8. Nourbakhsh, A. et al. MoS2 field-effect transistor with sub-10 nm channel length. Nano letters 16, 7798-7806 (2016).
9. Wu, K., Ma, H., Gao, Y., Hu, W. & Yang, J. Highly-efficient heterojunction solar cells based on two-dimensional tellurene and transition metal dichalcogenides. Journal of Materials Chemistry A 7, 7430-7436 (2019).
10. Wen, P. et al. Gate-Tunable Photovoltaic Effect in MoTe2 Lateral Homojunction. Advanced Electronic Materials, 2101144 (2021).
11. Withers, F. et al. Light-emitting diodes by band-structure engineering in van der Waals heterostructures. Nature materials 14, 301-306 (2015).

12. Geim, A. K. & Grigorieva, I. V. Van der Waals heterostructures. Nature 499, 419-425 (2013).
13. Pezeshki, A., Shokouh, S. H. H., Nazari, T., Oh, K. & Im, S. Electric and photovoltaic behavior of a few-layer α-MoTe2/MoS2 dichalcogenide heterojunction. Advanced Materials 28, 3216-3222 (2016).
14. Fathipour, S. et al. Exfoliated multilayer MoTe2 field-effect transistors. Applied Physics Letters 105, 192101 (2014).
15. Ahmed, F. et al. Multilayer MoTe2 Field-Effect Transistor at High Temperatures. Advanced Materials Interfaces 8, 2100950 (2021).
16. Han, X. et al. Multi-wavelength solitons delivered by an evanescent-field device based on polarization-sensitive MoTe 2 micro-sheets. Optical Materials Express 11, 3780-3791 (2021).
17. Schmidt, H., Giustiniano, F. & Eda, G. Electronic transport properties of transition metal dichalcogenide field-effect devices: surface and interface effects. Chemical Society Reviews 44, 7715-7736 (2015).
18. Marini, G. & Calandra, M. Light-Tunable Charge Density Wave Orders in MoTe 2 and WTe 2 Single Layers. Physical Review Letters 127, 257401 (2021).
19. Nakaharai, S., Yamamoto, M., Ueno, K. & Tsukagoshi, K. Carrier polarity control in α-MoTe2 Schottky junctions based on weak Fermi-level pinning. ACS applied materials & interfaces 8, 14732-14739 (2016).
20. Yu, W. J. et al. Highly efficient gate-tunable photocurrent generation in vertical heterostructures of layered materials. Nature nanotechnology 8, 952-958 (2013).
21. Lopez-Sanchez, O., Lembke, D., Kayci, M., Radenovic, A. & Kis, A. Ultrasensitive photodetectors based on monolayer MoS 2. Nature nanotechnology 8, 497-501 (2013).
22. Ghimire, M. K. et al. Defect-affected photocurrent in MoTe2 FETs. ACS applied materials & interfaces 11, 10068-10073 (2019).
23. Choi, H. et al. Edge contact for carrier injection and transport in MoS2 field-effect transistors. ACS nano 13, 13169-13175 (2019).
24. Liu, Y. et al. Approaching the Schottky–Mott limit in van der Waals metal–semiconductor junctions. Nature 557, 696-700 (2018).
25. Parto, K. et al. One-Dimensional Edge Contacts to Two-Dimensional Transition-Metal Dichalcogenides: Uncovering the Role of Schottky-Barrier Anisotropy in Charge Transport across Mo S 2/Metal Interfaces. Physical Review Applied 15, 064068 (2021).
26. Wang, Z. et al. MoTe 2: a type-II Weyl topological metal. Physical review letters 117, 056805 (2016).
27. Aftab, S. et al. Formation of an MoTe 2 based Schottky junction employing ultra-low and high resistive metal contacts. RSC advances 9, 10017-10023 (2019).
28. Kuiri, M. et al. Enhancing photoresponsivity using MoTe2-graphene vertical heterostructures. Applied Physics Letters 108, 063506 (2016).
29. Zhu, X., Wang, L. & Chen, L. Adsorption and dissociation of O 2 on MoSe 2 and MoTe 2 monolayers: ab initio study. International Journal of Modern Physics B 28, 1450195 (2014).
30. Zhang, Y. et al. Photothermoelectric and photovoltaic effects both present in MoS 2. Scientific reports 5, 1-7 (2015).